Nanoscale Advances

ROYAL SOCIETY OF CHEMISTRY

PAPER

View Article Online
View Journal | View Issue

Cite this: *Nanoscale Adv.*, 2025, **7**, 3558

Quantification of cellular uptake of gold nanoparticles *via* scattering intensity changes in flow cytometry†

Hye Ji Shin,[ab] Minjeong Kwak,[c] Ik Hwan Kwon,[c] Sook Heun Kim[d] and Ji Youn Lee *[ab]

Quantifying cellular uptake of nanoparticles is critical for understanding their biological interactions and optimizing their applications in nanomedicine. In this study, we developed a flow cytometry-based method to quantify the uptake of gold nanoparticles (AuNPs) using A549 cells. Taking advantage of the scattering properties of AuNPs, this method uses side scatter intensity to estimate the number of nanoparticles internalized by cells. However, directly measuring the exact number of internalized nanoparticles remains challenging due to the tendency of AuNPs to aggregate within cells. To address this, we introduce a new unit, molecules of equivalent gold nanoparticle (MEAuNP), which expresses side scatter intensity as a standardized unit based on the scattering of a single AuNP. While this method does not directly solve the problem of accurately measuring the exact number of internalized nanoparticles, it provides a semi-quantitative approach for estimating nanoparticle uptake. The obtained MEAuNP values are consistent with literature reports, suggesting that the approach yields reliable and comparable data. Moreover, the use of calibrated values ensures that consistent results can be obtained across different acquisition settings and potentially across different instruments. We further examined uptake dynamics and validated the method across multiple cell lines including HeLa, Beas-2B, Jurkat, and RPMI8226. This approach provides a robust tool for quantifying metal nanoparticle uptake, supporting the standardization of estimating uptake levels in various biological systems.

Received 6th November 2024
Accepted 10th April 2025

DOI: 10.1039/d4na00918e

rsc.li/nanoscale-advances

Introduction

Nanotechnology's growing impact across various sectors encompassing medicine,[1] food,[2] energy and environmental science,[3] and cosmetics[4] stems from its wide-ranging applications. For most biological applications, whether in biomedical endeavors to validate the effectiveness of nanomedicine or environmental studies examining the safety of engineered nanomaterials, quantifying cellular uptake is essential to understand nanoparticle function. Uptake is influenced by numerous factors, including physical attributes such as size and shape, chemical properties such as surface charge and modifications, and characteristics of the dispersion media such as the presence of serum proteins and temperature variations.[5–7]

Various methods are employed to quantify nanoparticle uptake, each offering unique advantages and challenges.[8,9] Transmission electron microscopy (TEM) provides high-resolution imaging capabilities, enabling direct visualization of nanoparticles and their interactions with cells.[10–12] Inductively coupled plasma (ICP)-based techniques offer highly quantitative measurements of nanoparticle content within cells but are destructive and limited to metal particles.[13,14] Nondestructive methods are also employed, as the intense light scattering that metal nanoparticles exhibit makes them suitable for investigating cellular uptake through dark-field microscopy, often combined with fluorescence microscopy to visualize cellular structures.[15,16] Due to the resolution limitations of light microscopy, nanoparticle detection is possible, but there are challenges in visualizing single nanoparticles. Despite this, light microscopy can still be useful for localization studies and, when combined with confocal microscopy, can provide three-dimensional information. Fluorescence-based techniques, such as flow cytometry and confocal microscopy, enable sensitive detection and quantification of fluorescently labeled

[a]*Biometrology Group, Division of Biomedical Metrology, Korea Research Institute of Standards and Science, 267 Gajeong-ro, Yuseong-gu, Daejeon 34113, Republic of Korea. E-mail: jylee@kriss.re.kr*

[b]*Graduate School of Analytical Science and Technology, Chungnam National University, 99 Daehak-ro, Yuseong-gu, Daejeon 34134, Republic of Korea*

[c]*Nanobio Measurement Group, Division of Biomedical Metrology, Korea Research Institute of Standards and Science, 267 Gajeong-ro, Yuseong-gu, Daejeon 34113, Republic of Korea*

[d]*Inorganic Metrology Group, Division of Chemical and Materials Metrology, Korea Research Institute of Standards and Science, 267 Gajeong-ro, Yuseong-gu, Daejeon 34113, Republic of Korea*

† Electronic supplementary information (ESI) available. See DOI: https://doi.org/10.1039/d4na00918e

nanoparticles in cells, offering insights into cellular uptake dynamics.[17,18] Additionally, microplate readers provide a high-throughput option for quantifying nanoparticle uptake, though they lack spatial information.[19] However, these developed techniques are only applicable to fluorescent nanoparticles. The inherent limitations of each method above necessitate the integration of complementary approaches to achieve comprehensive and reliable quantification of nanoparticle uptake. Integrating multiple techniques not only enhances the robustness of measurements but also provides insights into the complex mechanisms underlying nanoparticle–cell interactions.[17]

Gold nanoparticles (AuNPs) have shown promise for a multitude of biomedical and other applications owing to their unique physicochemical properties and versatile functionalities.[20] Their biocompatibility, tunable size and shape, and facile surface functionalization make them ideal candidates for targeted drug delivery, imaging, diagnostics, and therapy.[14,21] The ability to engineer AuNPs with tailored properties further accentuates their versatility and paves the way for innovative solutions to pressing societal challenges.[22] Importantly, they possess unique optical properties, characterized by high reflectivity and strong scattering of light. Taking advantage of these properties, flow cytometry offers a powerful tool for quantifying the cellular uptake of AuNPs that avoids the pitfalls of other methods, such as elaborate sample preparation and time-consuming and destructive analysis.

Flow cytometers measure both forward and side scatter, with side scatter being particularly sensitive to changes caused by metal nanoparticles within cells. The presence of metal nanoparticles significantly increases side scatter intensity, and efforts have been made to use this as a direct and quantitative measure of nanoparticle uptake.[16,23–28] By monitoring the increase in side scatter intensity, flow cytometry enables the quantification of nanoparticle uptake in mammalian cells, which facilitates the evaluation of uptake dynamics and nanoparticle–cell interactions. Unlike most methods to analyze the cellular uptake of nanoparticles, flow cytometry allows nondestructive analysis, meaning that the cells can be further sorted and used for other applications. In terms of AuNPs, one previous study was able to estimate the number of nanoparticles from scatter intensity by using empirical relationships between the amount of cellular AuNPs measured with ICP-mass spectrometry (MS) and side scatter intensities measured with a flow cytometer.[23] Furthermore, even home-built flow cytometers have demonstrated the capability for AuNP sizing and counting,[29] indicating the potential for diverse applications. Additionally, for metal nanoparticles such as silver and gold, their high scattering intensity makes them directly analyzable by flow cytometry.[30]

In this study, we aim to simply yet precisely quantify the number of AuNPs internalized within cells by utilizing the scatter intensity of single particles without the need for other quantitative methods. To achieve this, we employ a calibration curve between the side scatter intensity of single AuNPs and the voltage of the photomultiplier tube (PMT) detector. By establishing a correlation between scatter intensity and particle number, we provide a novel approach for quantifying AuNP uptake in cells. This methodology holds promise for enhancing our understanding of cellular interactions with nanoparticles and may contribute to the development of more effective nanoparticle-based therapeutics and diagnostics.

Materials and methods

Characterization of AuNPs

For the uptake analysis, a 90 nm AuNP certified reference material (CRM) (301-01-004, Korea Research Institute of Standards and Science) was used, in which the nanoparticles are dispersed in water containing a trace amount of sodium citrate. For the measurement of optical properties, UV-visible spectra were obtained from 350 to 900 nm using a spectrophotometer (UV-1800, Shimadzu). The particle size distribution by dynamic light scattering (DLS) was measured with a Zetasizer Nano ZSP (Malvern, UK). Scanning electron microscopy (SEM) images of the nanoparticles were obtained using a GeminiSEM 500 (Zeiss, Germany).

Cell culture

A549, RPMI8226, and Jurkat cells were maintained in RPMI 1640 supplemented with 10% fetal bovine serum (FBS), 200 units per mL penicillin, and 200 units per mL streptomycin. Beas-2B and HeLa cells were maintained in DMEM supplemented with 10% FBS, 200 units per mL penicillin, and 200 units per mL streptomycin. All cells were incubated at 37 °C in a humidified 5% CO_2 atmosphere. All cell lines were obtained from ATCC (American Type Culture Collection). Phase contrast and bright-field images were obtained using an inverted microscope (Olympus IX71). Routine cell counting and the viability assay were performed with a Countess II FL (Invitrogen) using the trypan blue exclusion method. All culture supplies were obtained from Thermo Fisher Scientific, unless otherwise indicated.

For the adherent cells (A549, Beas-2B, and HeLa), cells were seeded in 6-well plates at a density of 1×10^4 cells per cm^2. The following day, the culture medium was replaced with a fresh medium and used for nanoparticle treatment. For the suspension cells (Jurkat and RPMI8226), cells were maintained not exceeding 1–2 $\times$ 10^6 cells per mL and avoiding medium acidification, and an appropriate number of cells were prepared before the nanoparticle treatment.

Nanoparticle treatment

To ensure particle dispersion, AuNPs were sonicated before diluting them with culture media without FBS. To prevent potential degradation of serum proteins, FBS was added after the sonication step. The degree of dispersion and particle concentration were measured with UV-vis spectrometry. For the adherent cells, an appropriate volume of concentrated AuNPs prepared in the culture medium was added and mixed by gentle agitation by hand. For the suspension cells, 2×10^5 cells per well were seeded in a 6-well plate and then an appropriate volume of concentrated AuNP solution was added.

For the routine assay, after 18 h, cells were harvested and washed twice with a sufficient volume of 1× phosphate buffered saline (PBS) to remove residual nanoparticles both in the culture media and on the cell surfaces. The cells from each well were resuspended in approximately 0.5 mL of 1× PBS and kept at 4 °C before further analyses. To test various acquisition conditions, cells were treated with 5 and 10 μg mL^{-1} AuNP solution and then harvested at 18 h and prepared for analysis. For the kinetics assay, cells were treated with 10 μg mL^{-1} AuNP solution and harvested at 2, 4, 8, 20, and 24 h and prepared for analysis.

Nanoparticle uptake analysis using flow cytometry

Cells were analyzed using a FACSVerse™ (BD Biosciences). Before the analysis, 7-AAD (BioLegend) was added to the cell solution for a viability analysis. As routine acquisition, the side scatter (SSC) PMT detector voltage was set to 330 V. To test various acquisition conditions, the PMT voltage was adjusted in increments of 5 V ranging from 320 to 340 V. The acquisition settings, including the voltage of each channel except SSC, remained the same for all experiments. Live single cells were gated in a scatter plot after excluding cell debris and doublets, and its SSC histogram was used for analysis. All data were analyzed using FlowJo (version 10.9, FlowJo LLC).

Nanoparticle number concentration measurement using flow cytometry

A 100-fold diluted 90 nm AuNP solution was prepared by diluting the AuNP stock solution with a dilution buffer (20 nm filtered deionized water). The actual dilution fraction of each solution was determined by measuring its weight with an analytical balance. The concentration of AuNPs was measured at least three times using an Apogee Micro system (Apogee Flow Systems). Briefly, the AuNP population was gated in a plot of two side scatter channels, called middle angle light scattering (MALS) and large angle light scattering (LALS), to include the main population and exclude noise events identified by analyzing a dilution buffer control under the same setting.

Visualization of the nanoparticle location using bright-field and dark-field microscopy

Bright-field images of the cells were obtained using an IX71 inverted microscope, and dark-field images were captured with an enhanced dark-field microscope system (CytoViva). This system was customized to incorporate an objective lens (LMPLFLN100XBD, NA 0.9, Olympus) with an annulus condenser lens to achieve high-resolution dark-field imaging. A white-light LED (SOLIS-1D, Thorlabs) was used as a light source. Images were captured with a color CMOS camera (GS3-U3-51S5C-C, FLIR Grasshopper, Teledyne) at a resolution of 2048 × 2048 pixels with a pixel width of 5.5 μm. The system's magnification was configured to 100× using the objective lens in combination with a tube lens (TTL180-A, Thorlabs). Prior to dark-field imaging, cells were stained with CellTracker™ Orange to clearly visualize the cell-covered area. Fluorescence images were captured in the same field of view using RFP filter combinations with an enhanced dark-field microscopy system. Specifically, an excitation filter (Zeiss, 447748-4801) was placed in front of the condenser with a wavelength range of 550–650 nm, while an emission filter (Zeiss, 447714-8002) was positioned in front of the detector with a wavelength range of 585–615 nm.

Results and discussion

Quantification of nanoparticle uptake in A549 cells by flow cytometry

In the nanoparticle uptake experiments, we used AuNPs of 90 nm, developed as a CRM for a size standard. Their size measured by different methods showed high consistency between 85.8 and 94.7 nm, as displayed in Fig. 1. Considering that the equivalent circular diameter (ECD) represents a lower boundary due to the slightly angular shape of the AuNPs and that the Feret diameter represents an upper boundary by definition, the size measured by DLS fell within this range as expected. The UV-vis spectrum shows a distinct peak at around 555 nm, indicating that the AuNPs were monodisperse, which could be further confirmed by the DLS size distribution, with a polydispersity index value of 0.068. Also, the scatter plot obtained with a nanoflow cytometer and the high magnification dark-field image of AuNPs corroborate their monodisperse characteristics. SEM images reveal that the AuNPs had a slightly angular shape and were well dispersed as individual particles.

We treated A549 cells with AuNPs in a conventional upright configuration, where cells are placed on the bottom of the plate and a nanoparticle solution is added to the culture medium. Considering a rough division time of 24 h, we harvested cells 18 h after the treatment to minimize the dilution effect by cell division. Initially we tested nanoparticle concentrations from 1 to 30 μg mL^{-1} under serum-containing conditions. The presence of nanoparticles, at concentrations as high as 30 μg mL^{-1}, did not affect cell morphology, adhesion, or proliferation, with viability remaining high throughout the culture period (Fig. S1†). However, we could observe a large increase in side scatter from gated live single AuNP-treated cells in a concentration-dependent manner, while the forward scatter of A549 cells, which reflects their size, remained unchanged or slightly decreased as shown in Fig. 2A and B. These results are consistent with previously reported data on the cellular uptake of TiO_2 nanoparticles.[27]

As expected from the UV-vis spectrum of AuNPs in Fig. 1, which shows a peak at around 555 nm, the AuNP suspension displayed a purple-like color. The uptake of AuNPs was easily confirmed by the color of the cell pellet and was visible in a bright-field image (Fig. S2A†). Aggregated or agglomerated AuNPs appeared bluish purple and were mainly observed around the nucleus. We further imaged the cells using dark-field microscopy, a label-free imaging technique that enhances contrast in unstained samples, making it ideal for visualizing nanoparticles within biological specimens, especially metal nanoparticles with high reflectivity. Zucker *et al.* demonstrated that dark-field imaging is a powerful tool to analyze metal nanoparticle uptake in combination with flow

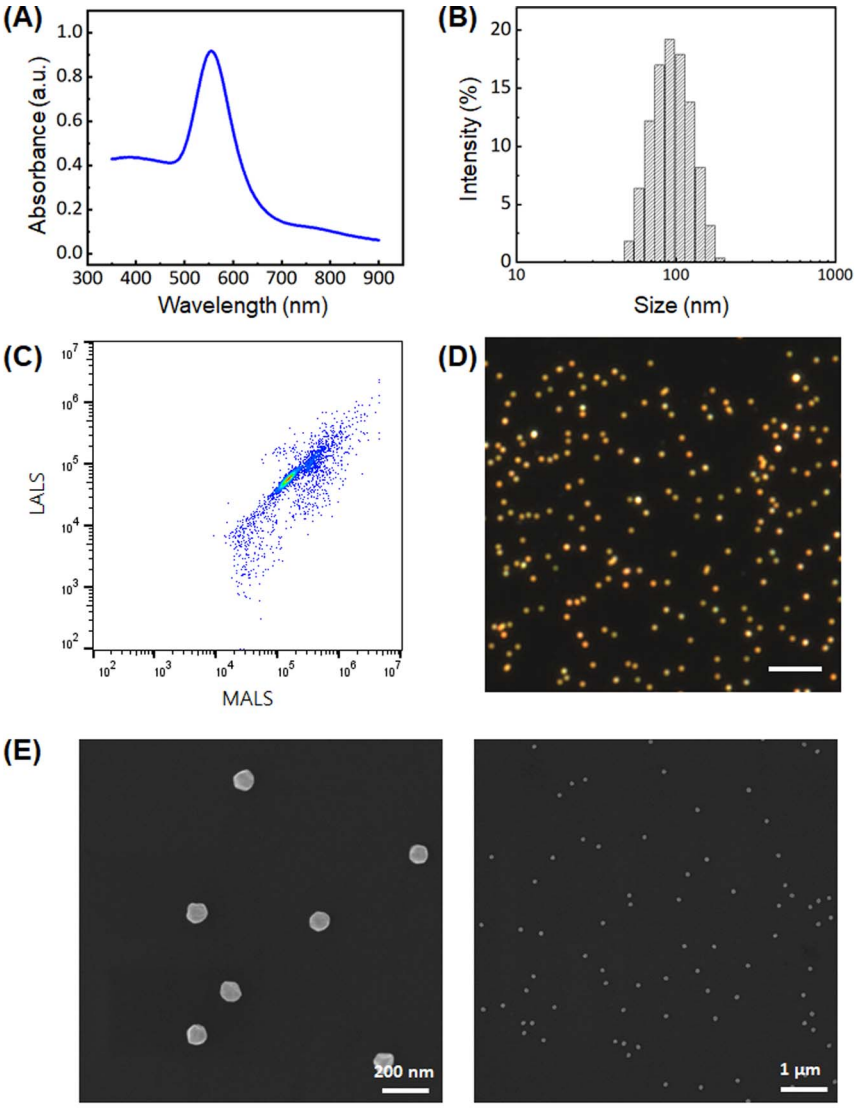

(F)

Measurement method	Certified value	Measurement uncertainty (k=2)
Transmission Electron Microscopy	85.8 nm (ECD*)	2.2 nm
	94.7 nm (Feret diameter)	2.4 nm
Dynamic Light Scattering	87.3 nm	2.5 nm

Fig. 1 Characterization and size analysis of AuNPs. (A) UV-vis absorption spectrum, (B) DLS size histogram, (C) scatter plot obtained using an Apogee flow cytometer, (D) dark-field image obtained with a 100× lens, and (E) SEM images at different magnifications (50 K and 10 K, working distance 5 mm), showing uniformity of the nanoparticle shape and size. (F) Certified size values for the AuNPs. *ECD: equivalent circular diameter.

cytometry.[16,24] AuNP-treated cells contained numerous bright yellow spots, indicating the presence of gold nanoparticles (Fig. 2C and S2B†). The dark-field images suggest that the AuNPs were internalized and mainly resided in subcellular components near the nuclei. It is known that a significant portion of nanoparticles accumulates in lysosomes 8–24 h post-uptake.[31–33] Since lysosomes are predominantly located in the perinuclear region, we hypothesize that the bright scattering observed near the nuclei in our images can be well explained by the accumulation of AuNPs in these organelles.

After confirming the ability to quantitatively analyze uptake using SSC intensity and the localization of AuNPs in cells, we conducted repeated experiments to assess intermediate precision. Triplicate experiments were performed within the concentration range of 1–16 μg per mL, which corresponds to 1.6×10^8 to 2.5×10^9 per mL, and these experiments were repeated on different days. The results from five independent experiments, depicted in Fig. 2B, exhibit concentration-dependent SSC intensity with good reproducibility, considering the inherent variation of biological samples. Factors

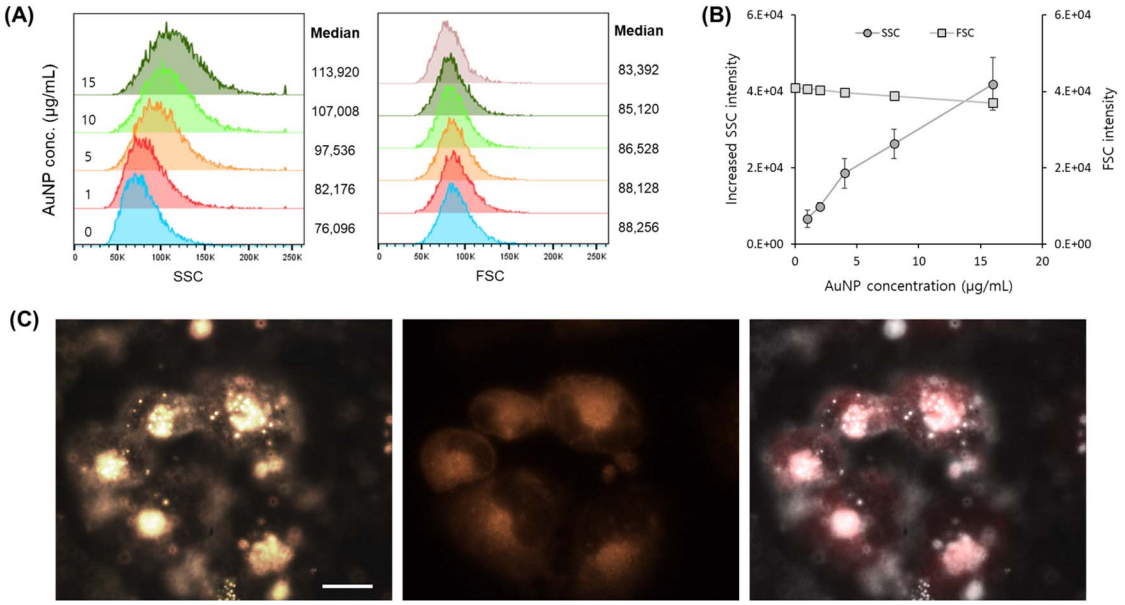

Fig. 2 AuNP uptake analysis in A549 cells with a flow cytometer and microscopies. (A) Exemplary SSC and FSC histograms with respective median values showing an increase in SSC intensity and no significant change in cell size distribution, respectively, in response to increasing concentrations of AuNPs (1, 5, 10, and 15 μg mL^{-1}). (B) AuNP concentration-dependent changes in SSC intensity and FSC intensity, demonstrating high reproducibility of the measurements. (C) Visualization of AuNP uptake with dark-field imaging. (Left) dark-field microscopy image highlighting AuNPs as bright yellow spots within the cells. (Middle) fluorescence images of stained cells marking the cell membrane and revealing the overall cell morphology. (Right) overlaid image. Scale bar = 20 μm.

influencing reproducibility include the cell condition, seeding density (cell confluency), sample preparation (including washing steps involving centrifugation), and variations in SSC intensity at the same voltage setting.

This result aligns with previous findings that showed an increase in SSC intensity upon cellular uptake of metal nanoparticles.[23,24] Given that side scatter is sensitive to variations in the refractive index and particle shape[34] and that metallic nanomaterials scatter light with high intensity relative to their size,[24] utilizing SSC intensity in flow cytometry provides a reliable method for analyzing the cellular uptake of AuNPs. However, most analyses remain qualitative rather than quantitative, as light intensity is often expressed in arbitrary units depending on the acquisition settings. Therefore, in this work, we aimed to express the increase in SSC intensity due to cellular uptake in an objective manner—specifically, by relating it to the scattering intensity of a single gold nanoparticle.

Measurement of SSC intensity of a single AuNP and molecules of equivalent AuNP (MEAuNP)

In the previous section, we found a concentration-dependent increase in SSC intensity upon cellular uptake of AuNPs, but only in arbitrary units. Next, we aimed to assess the feasibility of measuring the SSC intensity of individual AuNPs in order to correlate the increased intensity with the number of internalized nanoparticles. Owing to their high reflectivity, 90 nm AuNPs exhibit a distinct population in a cytogram of SSC *vs.* FSC intensity (Fig. 3A). Although the signal from the AuNPs was not entirely isolated from the background signal, the relatively low level of noise was insignificant as we could identify a distinctive population in the cytogram. Additionally, the AuNPs we used were developed as a size standard, making their size highly monodisperse with measurement uncertainty less than 3% of the certified value. This enabled us to confidently determine the representative SSC intensity value of single AuNPs.

However, a challenge arose when attempting to measure the scattering intensity of the AuNPs and A549 cells using the same settings. Despite the substantially greater scattering exhibited by AuNPs compared to cells, their significant size disparity (Fig. S3†) and the limited dynamic range of the PMT detector posed a constraint. At voltage settings suitable for cell measurement, the scattering intensity of the AuNPs was too low to be measured. Consequently, we investigated the possibility of extrapolating the SSC intensity value at the voltage used for cell measurements from the SSC intensity of AuNPs across varying voltages.

We systematically varied the voltage settings of the PMT detector from 380 to 500 V in 20 V increments to evaluate the SSC intensity of the AuNPs and investigate the potential for extrapolation. Our analysis revealed a strong correlation and a well-fitted exponential function between the PMT voltage and median SSC intensity values. As the SSC signal of AuNPs at 380 V was close to the threshold value, we established calibration parameters by measuring the SSC intensity at five points between 390 V and 460 V (Fig. 3B and C). Through repeated experiments, we consistently observed reproducible results, enabling us to assign the SSC intensity value of a single AuNP at 330 V, the voltage designated for cell measurements. This value facilitates the conversion of increased SSC intensity to the

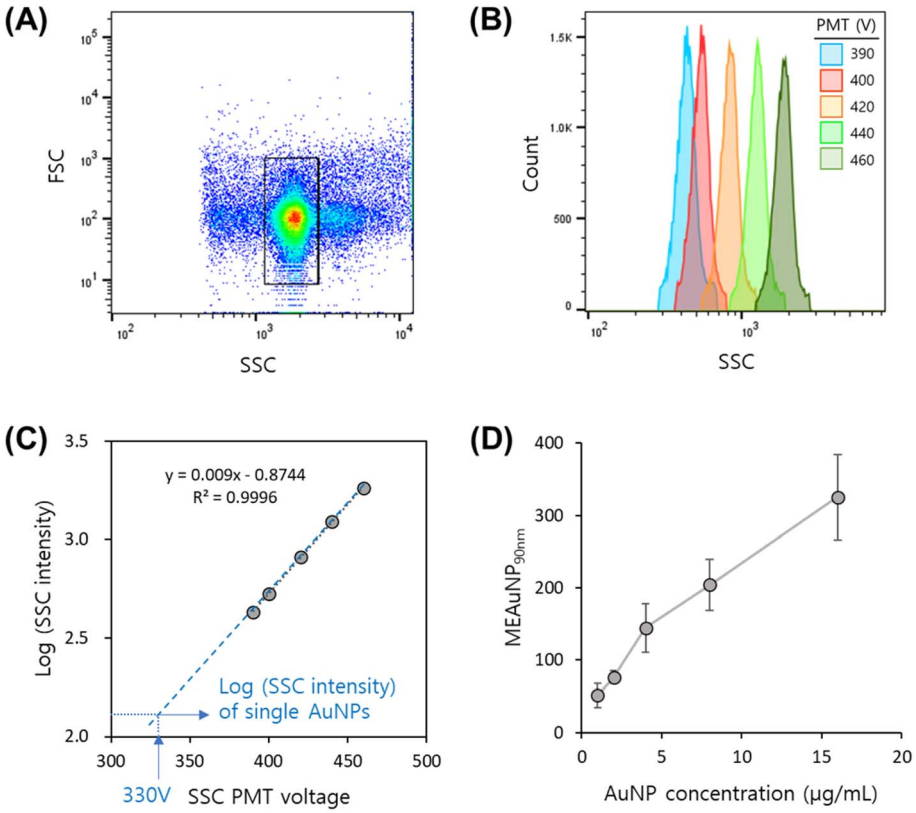

(E)

Method	Size (nm)	Treatment		# of particles /cell	Cell line	Ref.
		Concentration	Time (hr)			
ICP-MS	15	120 pM	24	29800	SK-BR-3	[39]
	54	20 pM		7100		
	100	2.8 pM		600		
ICP-MS	40	5 μg/mL	24	789	HeLa	[23]
	60			1501		
	80			429		
	100			181		
TEM	14	7x10^9/mL	24	1500	HeLa	[12]
	50			6000		
	74			3000		
ICP-AES	14	1x10^{10}/dish (6well dish)	14	850	MDA-MB-231	[14]
	50			1600		

Fig. 3 Estimation of SSC intensity of single AuNPs by extrapolation and conversion of increased SSC intensity into MEAuNP per cell. (A) Flow cytometry scatter plot (FSC *vs.* SSC) showing the gating of single AuNPs. (B) SSC intensity histograms of AuNPs at different PMT voltages, and (C) their logarithmic plot as a function of PMT voltage, showing a strong linear correlation ($R^2 = 0.9996$). The SSC intensity at 330 V where cell measurements were performed was extrapolated from the regression curve. (D) Plot of MEAuNP per cell as a function of AuNP concentration. Error bars represent the standard deviation ($n = 5$). (E) Summary of AuNP uptake levels reported in the literature.

intensity of single AuNPs and potentially allows for an estimation of the number of AuNPs present within the cells.

Although we successfully measured the SSC intensity of both single AuNPs and AuNP-treated A549 cells, it is challenging to directly calculate the number of AuNPs taken up by cells in practice. While the scatter intensity of micro-sized particles generally correlates with size to some extent, this relationship is not necessarily straightforward.[35] For AuNPs, the scattering intensity is influenced by various factors such as plasmon resonance, making it difficult to predict the scatter intensity based on size or amount alone. For a feasible conversion from the increase in SSC intensity to the number of AuNPs per cell, several assumptions must hold true, as follows. First, AuNPs exist as single particles both in culture media and in cells.

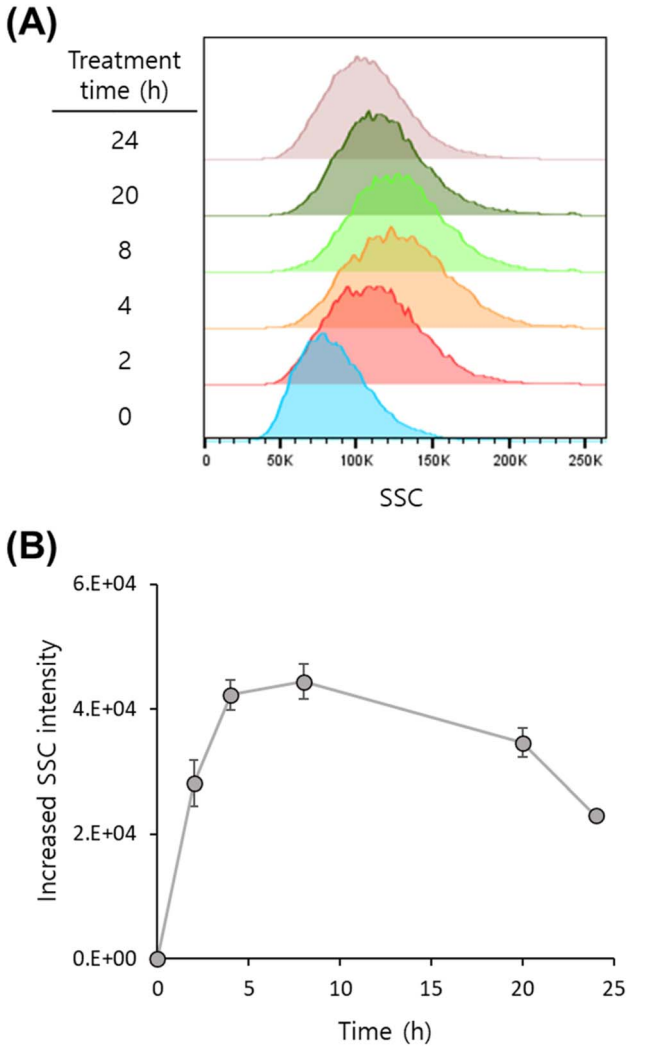

Fig. 4 Uptake kinetics of AuNPs in A549 cells analyzed by flow cytometry. (A) Histogram overlays of SSC intensity at various treatment times illustrating dynamic changes in AuNP uptake. (B) Graph showing a positively skewed uptake kinetics: an initial increase in SSC intensity with a peak at 4–6 h post-treatment followed by a gradual decrease.

Second, if AuNPs form aggregates or agglomerates, their scattering intensity is assumed to scale linearly with the number of particles in the aggregate—*i.e.*, an aggregate of n AuNPs would have n times the SSC intensity of a single nanoparticle. Third, the scattering intensity of AuNPs remains unchanged after being taken up by cells. Since these assumptions are unrealistic in most cases, we introduce a new unit termed molecules of equivalent gold nanoparticle, or MEAuNP. For this, we adapted the concept of molecules of equivalent soluble fluorophore (MESF) used for quantitative fluorescence measurements in flow cytometry.[36]

MESF translates fluorescence intensity into an equivalent number of fluorescent dye molecules, standardizing data across different instruments and conditions. This enables reliable comparisons of results, accurate quantification of molecules, and improved reproducibility. For practical applications, beads with assigned MESF values are used for calibration, which allows the fluorescence intensity from unknown samples to be converted into standardized MESF units. In our previous work, we demonstrated that MESF serves as an effective calibrator for estimating the cellular uptake of fluorescent nanoparticles with a flow cytometer, thus facilitating comparison across different experiments and reducing biological variability.[18] Similarly, MEAuNP can provide a standardized method for quantifying AuNP uptake in biological systems such as cells. As mentioned earlier, the scatter intensity is not strictly proportional to the amount of gold, meaning that the information regarding quantity is not perfectly accurate. Nevertheless, it provides a calibrated value, with which semi-quantitative information can be obtained.

We converted the increase in SSC intensity of AuNP-treated cells into MEAuNP and compared the values with those reported in the literature. The SSC intensity for single AuNPs at 330 V was consistently around 125. Using this value, we calculated the increased SSC intensity as MEAuNP, resulting in 50 to 320 MEAuNP for AuNP concentrations ranging from 1 to 16 μg mL^{-1} (approximately 0.3 to 4.2 pM) (Fig. 3D). To evaluate whether these values are relevant, we summarized the AuNP uptake levels reported in the literature, as shown in Fig. 3E, where most of the data were obtained using ICP-based methods and TEM and expressed as the number of particles per cell. While direct comparisons are difficult due to variations in nanoparticle size, surface modifications, and experimental conditions, particularly in treatment concentrations and times, the values we obtained are comparable to those reported in other studies. For example, as shown in Fig. 3E, in the case of 100 nm AuNPs, SK-BR-3 cells treated with 2.8 pM AuNPs showed an uptake of 600 particles per cell, while HeLa cells treated with 5 μg mL^{-1} AuNPs showed an uptake of 181 particles. Both cases reported values in the hundreds for a similar AuNP size and concentration to the current work, which aligns well with our experimental results.

Comparison of the results obtained from different acquisition settings

In the previous section, we demonstrated that the increase in SSC intensity in cells due to AuNP uptake could be calibrated using the SSC intensity of single AuNPs, expressed as MEAuNP. In the next experiment, measurements were initially conducted with a standardized setting, an SSC PMT voltage of 330 V, after which we investigated whether comparable results could be obtained under different measurement conditions by varying the PMT voltages during cell measurements and assessing the consistency of the results. Due to the large and complex nature of cells, even slight changes in SSC PMT voltage can lead to significant variations in intensity. Therefore, we adjusted the PMT voltage in 5 V increments, ranging from 320 to 340 V. The extrapolated intensity of single AuNPs was calculated at each voltage and used to convert the increased SSC intensity to MEAuNP. For A549 cells treated with 10 μg mL^{-1} AuNPs, the increased SSC intensity values ranged from approximately 25 500 to 41 500 across the different PMT voltages. However, the calculated MEAuNP remained consistent, ranging from 274 to

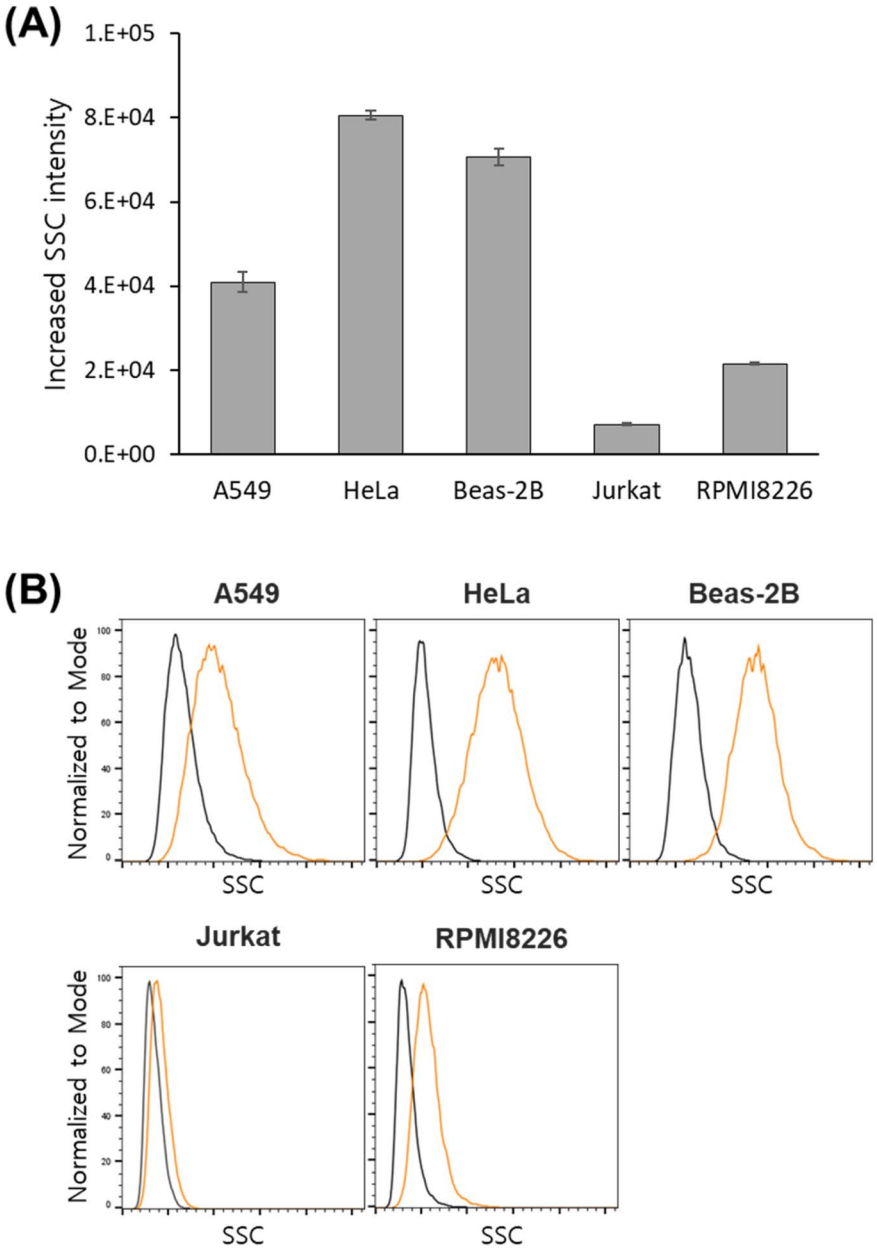

Fig. 5 Differential AuNP uptake across various cell lines. (A) Bar graph showing increased SSC intensity in response to AuNP treatment across five different cell lines. The results demonstrate significant variability in AuNP uptake between cell lines, with HeLa and A549 exhibiting the highest uptake and Jurkat and RPMI8226 showing considerably lower uptake. (B) SSC histograms comparing control (black) and AuNP-treated (orange) samples for each cell line. The shift in SSC intensity in AuNP-treated samples further highlights the differences in nanoparticle uptake among the cell lines.

295 particles with a % CV of about 3%. As shown in Fig. S4,† similar results were obtained across five independent experiments, with a % CV of less than 7%. Despite potential variations in cell conditions or confluency, the results were highly consistent, demonstrating that robust results can be achieved regardless of the measurement settings.

Kinetics of AuNP uptake in A549 cells

We also investigated the uptake dynamics of AuNPs in A549 cells by harvesting AuNP-treated cells at various time points and measuring the level of uptake. Unlike the uptake kinetics observed for silica or polystyrene nanoparticles in previous studies,[18,19] which typically showed either a continuous increase or a plateau after an initial increase, our results revealed a peak in uptake at 4–6 h post-treatment followed by a gradual decrease over time (Fig. 4). This trend also differs from other reports on the cellular uptake of AuNPs, where either a continuous increase or a plateau after an initial increase was observed.[37,38] We attribute this difference to variations in the size and concentration of the AuNPs used in our study compared to

those in the literature. Larger AuNPs likely exhibit faster sedimentation rates due to gravitational forces, leading to a greater dilution effect from cell division over time rather than continuous uptake. Sedimentation velocity calculation for 90 nm AuNPs yields approximately 1.31 mm per hour; considering a cell culture medium height of about 2 mm in the 6-well plate, this is a large value. Moreover, the impact of nanoparticle agglomeration and aggregation should also be considered potential factors influencing the observed uptake kinetics. Cho *et al.* systematically investigated the effects of sedimentation and diffusion on nanoparticle uptake by varying nanoparticle sizes and cell culture configurations.[39] Their study demonstrated that the impact of the configuration on uptake decreased with smaller AuNPs and became more pronounced as the particle size increased. This aligns with our observed uptake kinetics, suggesting that the high sedimentation rate of 90 nm AuNPs likely contributed to the unique uptake pattern observed in our study, namely a positively skewed curve.

Cellular uptake of AuNPs in other types of cells

To further demonstrate the versatility of the developed method, we quantified nanoparticle uptake in adherent cell lines (Beas-2B and HeLa) and suspension cell lines (Jurkat and RPMI8226) treated with 10 μg mL^{-1} AuNPs. Interestingly, the level of nanoparticle uptake varied as much as 12-fold among the tested cell lines, as shown in Fig. 5. Overall, the level of uptake was much higher in adherent cells, with HeLa showing the highest level of uptake followed by Beas-2B and A549. Jurkat and RPMI8226, on the other hand, showed a very limited level of uptake. As mentioned in the previous section, cellular uptake of AuNPs is significantly affected by sedimentation effects. Our previous study showed that the effective area interacting with the nanoparticles contributes more to uptake than tissue-specific differences, and the results of the current study suggest a similar cause.[18] For instance, Beas-2B cells, which have about a 1.3 times larger adhesion surface area than A549 cells, showed approximately 1.6 times more uptake of fluorescent silica nanoparticles. Likewise, in the present study, we observed that Beas-2B took up about 1.7 times more AuNPs than A549 cells. Suspension cells, which have a spherical shape, inherently have a smaller area for nanoparticle interaction compared to adherent cells.

Conclusions

In this study, we developed and validated a robust flow cytometry-based method for quantifying the cellular uptake of AuNPs by utilizing the side scatter intensity of AuNPs. Recognizing the challenge of directly measuring the number of internalized AuNPs due to their tendency to aggregate, we introduced the MEAuNP unit. This approach standardized SSC intensity based on the scattering properties of individual AuNPs, offering a practical solution for estimating nanoparticle uptake without assumptions about particle aggregation. The results demonstrated that the method provides consistent and comparable data across different acquisition settings, indicating its potential for application across various instruments. We also investigated nanoparticle uptake dynamics in A549 cells and validated the method across additional cell lines, namely HeLa, Beas-2B, Jurkat, and RPMI8226, confirming its versatility. Moreover, the proposed method is simple and efficient compared to other quantification techniques, as it requires no additional preprocessing, offers shorter processing times, and enables high-throughput analysis. Due to its nondestructive nature, this method can be combined with other quantification approaches to generate complementary data that can support a more comprehensive understanding of nanoparticle–cell interactions. The ability to quantify nanoparticle uptake in a standardized manner using flow cytometry provides significant advantages for nanomedicine research, presenting a practical, reproducible, and versatile tool for future studies.

Data availability

The data supporting this article have been included as part of the article or its ESI.†

Author contributions

Idea and study design: HJS, SHK, and JYL. Data generation and analysis: HJS for FCM and bright-field imaging data, MK for NP characterization, IHK for dark-field imaging data. Manuscript writing: HJS, SHK, and JYL.

Conflicts of interest

The authors declare no competing interests.

Acknowledgements

This work was supported by the Nano Material Technology Development Program (RS-2024-00452934) of the National Research Foundation and KRISS-GP2024-0006 from the Korea Research Institute of Standards and Science from the Ministry of Science and ICT. It was also supported by a National Research Council of Science & Technology grant (Project Number: GTL24021-500) by the Ministry of Science and ICT.

References

1 A. Ivask, A. J. Mitchell, A. Malysheva, N. H. Voelcker and E. Lombi, Methodologies and approaches for the analysis of cell–nanoparticle interactions, *WIREs Nanomed. Nanobiotechnol.*, 2018, **10**, e1486.
2 P. Sanguansri and M. A. Augustin, Nanoscale materials development - a food industry perspective, *Trends Food Sci. Technol.*, 2006, **17**, 547–556.
3 A. Kumar, P. Choudhary, A. Kumar, P. H. C. Camargo and V. Krishnan, Recent advances in plasmonic photocatalysis based on TiO_2 and noble metal nanoparticles for energy conversion, environmental remediation, and organic synthesis, *Small*, 2022, **18**, e2101638.

4 J. W. Wiechers and N. Musee, Engineered inorganic nanoparticles and cosmetics: Facts, issues, knowledge gaps and challenges, *J. Biomed. Nanotechnol.*, 2010, **6**, 408–431.
5 S. Behzadi, *et al.*, Cellular uptake of nanoparticles: journey inside the cell, *Chem. Soc. Rev.*, 2017, **46**, 4218–4244.
6 A. Lesniak, *et al.*, Effects of the presence or absence of a protein corona on silica nanoparticle uptake and impact on cells, *ACS Nano*, 2012, **6**, 5845–5857.
7 P. Rees, J. W. Wills, M. R. Brown, C. M. Barnes and H. D. Summers, The origin of heterogeneous nanoparticle uptake by cells, *Nat. Commun.*, 2019, **10**, 1–8.
8 A. Elsaesser, *et al.*, Quantification of nanoparticle uptake by cells using an unbiased sampling method and electron microscopy, *Nanomedicine*, 2011, **6**, 1189–1198.
9 D. Bobo, K. J. Robinson, J. Islam, K. J. Thurecht and S. R. Corrie, Nanoparticle-based medicines: a review of FDA-approved materials and clinical trials to date, *Pharm. Res.*, 2016, **33**, 2373–2387.
10 Z. Chu, Y. Huang, Q. Tao and Q. Li, Cellular uptake, evolution, and excretion of silica nanoparticles in human cells, *Nanoscale*, 2011, **3**, 3291–3299.
11 A. Kumar, A. K. Pandey, S. S. Singh, R. Shanker and A. Dhawan, A flow cytometric method to assess nanoparticle uptake in bacteria, *Cytometry, Part A*, 2011, **79A**, 707–712.
12 D. B. Chithrani, *et al.*, Gold nanoparticles as radiation sensitizers in cancer therapy, *Radiat. Res.*, 2010, **173**, 719–728.
13 J. Xie, C. Xu, N. Kohler, Y. Hou and S. Sun, Controlled PEGylation of monodisperse Fe_3O_4 nanoparticles for reduced non-specific uptake by macrophage cells, *Adv. Mater.*, 2007, **19**, 3163–3166.
14 C. Cruje, C. Yang, J. Uertz, M. Van Prooijen and B. D. Chithrani, Optimization of PEG coated nanoscale gold particles for enhanced radiation therapy, *RSC Adv.*, 2015, **5**, 101525–101532.
15 R. M. Zucker and K. M. Daniel, Microscopy imaging methods for the detection of silver and titanium nanoparticles within cells, in *Methods in Molecular Biology*, ed. Soloviev, M., Humana Press, 2012, vol. 906, pp. 483–496.
16 R. M. Zucker, J. Ortenzio, L. L. Degn, J. M. Lerner and K. Boyes, Biophysical comparison of four silver nanoparticles coatings using microscopy, hyperspectral imaging and flow cytometry, *PLoS One*, 2019, **14**, e0219078.
17 C. Gottstein, G. Wu, B. J. Wong and J. A. Zasadzinski, Precise quantification of nanoparticle internalization, *ACS Nano*, 2013, **7**, 4933–4945.
18 H. Shin, M. Kwak, T. G. Lee and J. Y. Lee, Quantifying the level of nanoparticle uptake in mammalian cells using flow cytometry, *Nanoscale*, 2020, **12**, 15743–15751.
19 H. J. Shin, M. Kwak, S. Joo and J. Y. Lee, Quantifying fluorescent nanoparticle uptake in mammalian cells using a plate reader, *Sci. Rep.*, 2022, 1–9, DOI: 10.1038/s41598-022-24480-3.
20 R. A. Sperling, P. R. Gil, F. Zhang, M. Zanella and W. J. Parak, Biological applications of gold nanoparticles, *Chem. Soc. Rev.*, 2008, **37**, 1896–1908.
21 M. S. Yavuz, *et al.*, Gold nanocages covered by smart polymers for controlled release with near-infrared light, *Nat. Mater.*, 2009, **8**, 935–939.
22 M. J. Mitchell, *et al.*, Engineering precision nanoparticles for drug delivery, *Nat. Rev. Drug Discovery*, 2021, **20**, 101–124.
23 J. Park, M. K. Ha, N. Yang and T. H. Yoon, Flow cytometry-based quantification of cellular Au nanoparticles, *Anal. Chem.*, 2017, **89**, 2449–2456.
24 R. M. Zucker, E. J. Massaro, K. M. Sanders, L. L. Degn and W. K. Boyes, Detection of TiO_2 nanoparticles in cells by flow cytometry, *Cytometry, Part A*, 2010, **77**, 677–685.
25 Y. Ibuki and T. Toyooka, Nanoparticle uptake measured by flow cytometry, in *Methods in Molecular Biology*, ed. J. Reineke, 2012, vol. 926, pp. 157–166.
26 Y. Wu, M. R. K. Ali, K. Dansby and M. A. El-sayed, Improving the flow cytometry-based detection of the cellular uptake of gold nanoparticles, *Anal. Chem.*, 2019, **91**, 14261–14267.
27 H. Suzuki, T. Toyooka and Y. Ibuki, Simple and easy method to evaluate uptake potential of nanoparticles in mammalian cells using a flow cytometric light scatter analysis, *Environ. Sci. Technol.*, 2007, **41**, 3018–3024.
28 R. M. Zucker, *et al.*, Detection of silver nanoparticles in cells by flow cytometry using light sScatter and far-red fluorescence, *Cytometry, Part A*, 2013, **83**, 962–972.
29 S. Zhu, *et al.*, Size differentiation and absolute quantification of gold nanoparticles *via* single particle detection with a laboratory-built high-sensitivity flow cytomter, *J. Am. Chem. Soc.*, 2010, **132**, 12176–12178.
30 R. M. Zucker, J. N. R. Ortenzio and W. K. Boyes, Characterization , Detection , and Counting of Metal Nanoparticles Using Flow Cytometry, *Cytometry, Part A*, 2016, **89**, 169–183.
31 L. Treuel, X. Jiang and G. U. Nienhaus, New views on cellular uptake and trafficking of manufactured nanoparticles, *J. R. Soc. Interface*, 2013, **10**, 20120939.
32 L. Wang, *et al.*, Selective targeting of gold nanorods at the mitochondria of cancer cells: Implications for cancer therapy, *Nano Lett.*, 2011, **11**, 772–780.
33 C. Dalal, A. Saha and N. R. Jana, Nanoparticle Multivalency Directed Shifting of Cellular Uptake Mechanism, *J. Phys. Chem. C*, 2016, **120**, 6778–6786.
34 G. C. Salzman, Light Scatter : Detection and Usage, *Curr. Protoc. Cytom.*, 1999, **1**(13), 1–8.
35 M. Hussels, H. Lichtenfeld, H. Woehlecke, E. Wollik and D. Lerche, Instrument with an ultra-wide dynamic detection range for the optical counting and sizing of individual particles in suspensions, *Rev. Sci. Instrum.*, 2024, **95**, 023704.
36 A. Schwartz, *et al.*, Quantitating fluorescence intensity from fluorophore: The definition of MESF assignment, *J. Res. Natl. Inst. Stand. Technol.*, 2002, **107**, 83–91.
37 L. C. Kennedy, *et al.*, T cells enhance gold nanoparticle delivery to tumors in vivo, *Nanoscale Res. Lett.*, 2011, **6**, 283.
38 B. D. Chithrani, A. A. Ghazani and W. C. W. Chan, Determining the size and shape dependence of gold nanoparticle uptake into mammalian cells, *Nano Lett.*, 2006, **6**, 662–668.
39 E. C. Cho, Q. Zhang and Y. Xia, The effect of sedimentation and diffusion on cellular uptake of gold nanoparticles, *Nat. Nanotechnol.*, 2011, **6**, 385–391.